

# FEASIBILITY OF ULTRA-LOW-DOSE MULTI-DETECTOR-ROW CT-COLONOGRAPHY: DETECTION OF ARTIFICIAL ENDOLUMINAL LESIONS IN AN IN-VITRO-MODEL WITH OPTIMIZATION OF IMAGE QUALITY USING A NOISE REDUCTION FILTER ALGORITHM

M. Branschofsky<sup>1</sup>, C. Vogt<sup>2</sup>, V. Aurich<sup>3</sup>, A. Beck<sup>3</sup>, U. Mödder<sup>1</sup>, M. Cohnen<sup>1</sup>

<sup>1</sup>Institute of Diagnostic Radiology, University Hospital Düsseldorf (Director: Prof. Dr. Ulrich Mödder)

<sup>2</sup>Department of Gastroenterology, Hepatology and Infectiology, University Hospital Düsseldorf (Director: Prof. Dr. Dieter Häussinger)

<sup>3</sup>Department of Informatics, Institute of Mathematics, Heinrich-Heine University Düsseldorf, (Director: Prof. Dr. Volker Aurich), Düsseldorf, Germany

## Abstract

*Purpose:* To assess the most favorable slice thickness in Multi-Detector-Row CT-colonography (MDCTC), and the feasibility of dose reduction in an in-vitro-setting as well as the possibility of optimization of image quality using a noise reduction filter algorithm.

*Materials and Methods:* 18 artificial lesions with sizes from 1 to 8 mm were randomly positioned in two cleansed pig colons. At a "Somatom Plus 4 Volume Zoom", six scanning protocols using a slice collimation of 2.5, 1, and 1 mm with a reconstructed slice thickness of 3, 3, and 1.25 mm were performed with tube currents of 100, and 10 mAs, respectively. Using a non-commercial software, a non-linear Gaussian filter was used to minimize image noise. Image noise was assessed before and after application of the filtering process. Using a threshold of -750 HU, two blinded readers analyzed the virtual colonography in respect to lesion location, size, and shape. Artifacts were noted. An automated detection system was evaluated.

*Results:* Using 10 mAs, a ten-fold dose reduction was achieved. After application of the mathematical filter, image noise was reduced by 45-80% for 100 mAs, and by 50-70% for 10 mAs scans. Only with a slice thickness of 1.25 mm, all lesions could be detected. The definition of lesion size and shape was more accurate with higher mAs. Only minor noise artifacts were noted on low-dose images. The automated polyp detector marked not more than 60% of artificial lesions.

*Conclusion:* MDCTC benefits from narrow slice collimation. In an in-vitro-model, a significant dose reduction is achievable with preservation of a high lesion detection rate. The noise reduction filter algorithm improved image quality substantially.

*Key words:* Colon, CT; Colon, Neoplasms; Computed Tomography, image processing; Computed Tomography, three-dimensional; Dose Reduction

*Abbreviations:* VCTC = Virtual CT-colonography, MDCT = Multi-Detector-Row CT, MDCTC = Multi-Detector-Row CT-colonography, ULD-MDCTC:

ultra-low-dose MDCTC, HU = Hounsfield unit, ROI = regions of interest, a.u. = arbitrary units

## INTRODUCTION

Since its first description, virtual CT colonography (VCTC) is a rapidly developing technique for non-invasive evaluation of the colon for polyps and tumors [1-4]. Many authors have shown that VCTC can reliably detect polyps and tumors of 1 cm size or more with a high sensitivity and specificity of more than 90% [5-7]. With the advent of Multi-Detector-Row CT (MDCT), an improvement of examination parameters bears the potential of an increased detection rate of endoluminal lesions [8-12]. In contrast, other studies did not reveal a substantial benefit of MDCT [13-15].

The detection of polyps smaller than 5 mm still remains the challenge for any non-invasive diagnostic method incapable of histologic confirmation. Especially in view of the new technical abilities of MDCT with rapid thin-slice imaging no general examination protocol has been defined as yet [16]. Particularly in view of a potential screening situation a dose reduction is warranted. Therefore the present study was designed to evaluate the feasibility of an ultra-low-dose protocol in a phantom setting. As image noise increases resulting from thin-slice and low-dose protocols thus lowering image quality, noise reduction filter algorithms could probably enhance image quality without affecting lesion detection or radiation dose.

The first studies on MDCT-colonography (MDCTC) have used a slice collimation varying from 4x1 to 4x5 mm with a resulting slice thickness varying from 3 to 5 mm [13-16]. Thus, the present study used a systematic variation of slice thickness in order to analyze the detection rate of artificial lesions.

The presented in-vitro-model was used to simulate an ultra-low-dose MDCTC (ULD-MDCTC) under ideal conditions without bowel or patient movement, fecal residue or haustral folds, and to define the best possible performance both on 2D-images as well as on 3D-reconstructions. Noise, according to image quality,

was investigated before and after the application of a mathematical noise filter algorithm.

As automated systems for computer aided detection of polyps begin to emerge in clinical routine, an automated polyp detection system was evaluated both on normal- as well as on low-dose-phantoms [17, 18].

### MATERIAL AND METHODS

Two cleansed pig colons of approximately 20- and 25-inch length (80-cm and 100-cm), respectively, were used as phantoms. In approximation to natural polyps, 18 differently shaped lesions (Table 1) were created from a special dental wax (Fig. 1).

Table 1. Number, size, and shape of the artificial lesions used in this study.

Type	Number	Surface	Size [mm]	Shape	Stalk
I	4	irregular	5 to 8	spheric	short
II	4	smooth	2 to 8	spheric	long
III	4	irregular	2 to 5	flat	-
IV	6	smooth	1 to 5	spheric	-

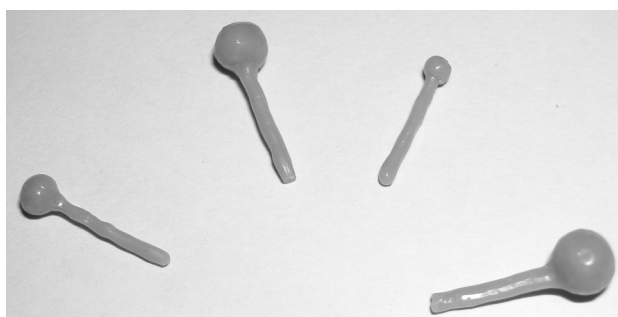


Fig. 1. Spheric lesions (long stalk).

The mean density of the lesions was -16 HU on 1 mm single slice scanning. Lesions were fixed in random order by one of us (M.B.) with cyanacryl-glye as 1 to 5 mm lesions are difficult to suture and a perforation of the thin colonic wall had to be avoided. After closure at one end, the two pig colons were inflated with room air by use of a plastic tube with insufflation balloon. The mean luminal diameter was 4 cm. Subsequently, the colons were totally emerged into a translucent plastic box (33 cm x 47 cm x 24 cm) containing a water-contrast-solution. This solution had a mean density of 14 HU after 100 cc of non-ionic contrast media (Solutrast™, Iopamidol with 300 mg iodine/ml; Schering, Berlin, Germany) were applied.

Six different examination protocols were performed at a MDCT scanner ("Somatom Plus 4 Volume Zoom", Software: "Somaris VA 20 Q"; both: Siemens, Erlangen, Germany) (Table 2). In "normal-dose" protocols, tube current was set to 100 mAs. For dose reduction, "low-dose" protocols with a tube current of 10 mAs were generated. This is the lowest setting achievable with the current software version.

Slice collimation was 4x1 mm with 1.25 mm slices as well as 3 mm slices being reconstructed. Secondly, a slice collimation of 4x2.5 mm with 3 mm slices were examined in addition. The increment was set constantly to 0.7 mm with a resulting overlap of 76.6% for 3 mm slices, and of 44% for 1.25 mm slices. The field of view was 35 cm to cover the box completely with an in plane resolution of 0.68 mm at a 512-matrix.

The implemented CT-scanner-software displays mean density and noise as standard deviation of density when ROI were placed within the source image. Density and noise for air surrounding the phantom, within the colonic lumen, within the water solution as well as in the lesions were determined using ROI placed in at least five different images. Data presented are the mean values (Table 4). For two- and three-dimensional analysis, data were transferred to a remote workstation (PC-system, 1 GHz Intel processor, 1 GB memory, LINUX). A dedicated software ("ECCET")

Table 2. Examination parameters of the six protocols performed. Slice collimation refers to the collimation of the primary beam. Slice thickness refers to the freely selectable thickness of resulting images.

	Protocol I	Protocol II	Protocol III	Protocol IV	Protocol V	Protocol VI
Slice collimat. [mm]	1	1	1	1	2.5	2.5
Slice thickness [mm]	1.25	1.25	3	3	3	3
Table feed [mm]	8	8	8	8	17.5	12.5
Pitch, "classical"	2	2	2	2	1.75	1.25
Tube current [mAs]	10	100	10	100	10	100
Tube voltage [kVp]	120	120	120	120	120	120
Rotation time [s]	0.5	0.5	0.5	0.5	0.5	0.5
Scan length [mm]	250	250	250	250	250	250
Scan time [s]	16.4	16.4	16.4	16.4	7.96	11.06
CTDI [mGy]	1.14	11.4	1.14	11.4	0.94	9.4
DLP [mGy x cm]	28.5	285	28.5	285	23.5	235

was developed by two of us (V.A., A.B.). Firstly, a non-linear Gaussian filter was used to minimize noise [19]. Secondly, the colonic lumen was automatically segmented using a threshold of  $-750$  HU, and a three-dimensional volume was generated. The "ECCT"-software allows a simultaneous visualization of 2D-images, 3D-reconstructions as well as virtual 3D-endoluminal perspective views including an online-ability to switch between 2D- and 3D-mode, and vice versa.

Using this system, the two pig colons were analyzed by two observers (M.C., C.V.) who were blinded to the location and order of lesions. Observers were asked to define the artificial polyps in location, size and shape with a consensus decision being reached in case of disagreement. In order to prevent acquaintance to the artificial lesions, each evaluation was at least three weeks apart from the other. Observers were asked to evaluate separately 2D-images with 3D-multiplanar reconstructions as opposed to 3D-endoluminal views. A deviation in size of more than 2 mm in one direction or 1 mm in two directions was defined as not correct.

After mathematical noise reduction, resulting images were recorded in similar projections as source images and stored in TIFF format. A non-commercial software ("SCION Image for Windows 2000 beta 4.0.2, Scion Corp., Maryland, USA) was used to evaluate density and noise defined as standard deviation of the mean density. Gray scale values were reduced to 256 arbitrary units, with 255 representing black, and 0 white, respectively. ROI-measurements as described above were performed both in filtered and unfiltered images separately.

Furthermore, artifacts were noted as well as quantified according to a subjective score (minor - barely visible; moderate - present, but not preventing lesion detection; marked - lesion detection is deteriorated).

After this assessment an automatic detection system was applied that marks any discrete lesion with an acute angle to the surrounding surface with a size of more than 3 pixels ( $= 2.1$  mm). The performance of this system in percent detected lesions was noted.

## RESULTS

Using the 1.25 mm slices of protocol I and II, all lesions could be detected both on 2D- as well as on 3D-images (Table 4). In protocols III and IV with a reconstructed slice thickness of 3 mm out of a 1 mm slice collimation, 17 of 18 lesions (94%) were found. One 1x1 mm spheric lesion was neither visible on 2D-images, 3D-reconstructions or 3D-endoluminal views. In 2D-images the other 1x1 mm lesion was detected by one observer. On 3D-reconstructions and 3D-endoluminal views both 1 mm lesions were invisible. In protocols V and VI, 16 of 18 lesions (89%) were clearly delineated. Both 1x1 mm spheric lesions could not be detected both on 2D-images and 3D-views.

The exact shape of lesions could be defined in more than 70% in low-dose protocols with a correct rate exceeding 80% for the normal-dose protocols. The smaller the reconstructed slice thickness, the better the rate was and reached 94% (protocol II).

Size estimation was correct in only about one half of lesions, a slight tendency towards a size underestimation was noted (Table 3).

The density of the water solution was constant for all protocols (Table 4). Noise was significantly lower for the protocols with broader slices and higher dose. Table 2 (referring to CTDI) and Table 4 illustrate that slice thickness had more influence on noise than dose. With constant CTDI, noise of the water solution increased from 34.3 to 43.9 HU when images with 1.25

*Table 3.* Rate of detection of endoluminal artificial lesions. Size was determined by electronic means. An over- or underestimation was assumed when a divergence of more than two millimeters in one direction or of one millimeters in two directions was found. "Polyp Detector": detection rate of the automated detection system.

	Protocol I	Protocol II	Protocol III	Protocol IV	Protocol V	Protocol VI
Rate of detection	100 %	100 %	94 %	94 %	88.8 %	88.8 %
Shape correct	77.8 %	94.4 %	72.2 %	88.8 %	77.8 %	83.3 %
Size correct	38.9 %	38.9 %	47.1 %	52.9 %	50 %	37.5 %
Size overestim.	38.9 %	33.3 %	47.1 %	29.4 %	25 %	31.3 %
Size underestim.	22.2 %	27.8 %	5.8 %	17.6 %	25 %	31.3 %
Polyp Detector	55 %	55 %	61 %	55 %	50 %	50 %

*Table 4.* Mean density and noise (standard deviation of density) in [HU] as determined by ROI-measurements in source images for different objects. The lesion density decreases with larger slice thickness due to volume averaging.

Density $\pm$ Noise [HU]	Protocol I	Protocol II	Protocol III	Protocol IV	Protocol V	Protocol VI
Air	$-996 \pm 22$	$-996 \pm 21$	$-997 \pm 18$	$-997 \pm 17$	$-997 \pm 16$	$-998 \pm 7$
Colonic lumen	$-992 \pm 29$	$-991 \pm 29$	$-995 \pm 24$	$-994 \pm 25$	$-989 \pm 25$	$-993 \pm 11$
Water solution	$14 \pm 47$	$14 \pm 44$	$14 \pm 39$	$14 \pm 34$	$13 \pm 32$	$14 \pm 11$
Lesion	$-25 \pm 37$	$-14 \pm 28$	$-30 \pm 31$	$-22 \pm 24$	$-67 \pm 24$	$-95 \pm 20$

Table 5. Density and SEM („noise“) as determined by a non-commercial program („SCION Image“) in images without mathematical noise filter (upper values) and in images after mathematical noise reduction (lower values - bold type). Arbitrary units on a scale ranging from 0 to 255.

Density $\pm$ Noise [a.u.] Values: unfiltered - <b>filtered</b>	Protocol I	Protocol II	Protocol III	Protocol IV	Protocol V	Protocol VI
Air	223.1 $\pm$ 2.4 <b>212.2 <math>\pm</math> 0.7</b>	223.5 $\pm$ 1.1 <b>212.6 <math>\pm</math> 0.5</b>	223. $\pm$ 2.1 <b>218.9 <math>\pm</math> 0.6</b>	223.5 $\pm$ 0.9 <b>212.6 <math>\pm</math> 0.5</b>	223.3 $\pm$ 1.8 <b>217.7 <math>\pm</math> 0.5</b>	223.3 $\pm$ 1.8 <b>217.6 <math>\pm</math> 0.6</b>
Colonic Lumen	222.5 $\pm$ 3.2 <b>211.8 <math>\pm</math> 1.2</b>	222.9 $\pm$ 1.5 <b>212.0 <math>\pm</math> 0.3</b>	222.7 $\pm$ 2.8 <b>218.5 <math>\pm</math> 0.9</b>	222.9 $\pm$ 1.2 <b>212.0 <math>\pm</math> 0.2</b>	222.4 $\pm$ 2.7 <b>216.6 <math>\pm</math> 0.9</b>	222.5 $\pm$ 2.6 <b>216.7 <math>\pm</math> 0.9</b>
Water solution	120.5 $\pm$ 5.0 <b>105.2 <math>\pm</math> 3.2</b>	120.7 $\pm$ 1.7 <b>95.9 <math>\pm</math> 0.4</b>	120.7 $\pm$ 4.1 <b>113.8 <math>\pm</math> 2.2</b>	120.6 $\pm$ 1.4 <b>113.9 <math>\pm</math> 0.3</b>	120.7 $\pm$ 3.7 <b>108.8 <math>\pm</math> 1.9</b>	120.7 $\pm$ 3.6 <b>108.7 <math>\pm</math> 1.9</b>
Lesion	131.0 $\pm$ 6.9 <b>114.2 <math>\pm</math> 3.9</b>	127.5 $\pm$ 2.5 <b>106.7 <math>\pm</math> 5.1</b>	129.7 $\pm$ 5.1 <b>125.9 <math>\pm</math> 4.2</b>	127.7 $\pm$ 1.8 <b>122.8 <math>\pm</math> 1.4</b>	134.1 $\pm$ 4.7 <b>125.9 <math>\pm</math> 3.6</b>	131.1 $\pm$ 1.3 <b>124.5 <math>\pm</math> 3.2</b>

mm are reconstructed as opposed to 3 mm (protocols II/IV). With a constant slice thickness of 1.25 mm, noise of the water solution increased only from 43.9 to 46.6 HU with a ten-fold reduction of tube current (protocols I/II). With the 2.5 mm collimation, this effect is more prominent, as noise increased from 11.3 to 32.2 HU. Both CTDI as well as DLP were reduced by a factor of ten after reduction of tube current from 100 to 10 mAs. The mean density of lesions was inconstant most likely due to volume averaging because of different slice collimations.

The mean gray scale values after ROI-analysis of the non-filtered source images are presented in Table 5 (upper values) as well as the mean gray scale values of the filtered images (lower values - bold type). For the measurements in air image noise in filtered images was constantly below 0.7 a.u. while in source images values of up to 2.4 a.u. were seen. Independent to slice thickness, the mean noise reduction by application of a non-linear Gaussian filter was between 50% to 70% for low-dose images, and 45% to 80% in normal dose images.

In normal dose 2D-images, 3D-reconstructions or 3D-endoluminal views, no noise-related artifacts were noted on subjective assessment. After mathematical noise reduction, the low-dose 3D-reconstructions and 3D-endoluminal views revealed only minor noise artifacts which appeared as single voxels of "snow" or "dust" in the colonic lumen. Elevating the cut-off threshold to -650 HU eliminated these artifacts completely.

Stairstep-artifacts were graded as minor for protocols I, II, IV, and VI, respectively. For protocols III and V, stairstep-artifacts were graded as moderate. Other artifacts were not noted.

The automated polyp detector marked between 50 and 60% of all artificial polyps as a discrete endoluminal lesion. The flat lesions as well as lesions smaller than 3 mm were not detected. False positive markers were not observed.

## DISCUSSION

The aim of the present study was to evaluate the feasibility of ULD-MDCTC in an in-vitro-setting. Additionally the influence of a mathematical noise filter algorithm on image quality should be evaluated. The in-vitro setting of this experiment using a resected and cleansed pig colon demonstrated that artificial endoluminal lesions from 1 to 8 mm size can reliably be detected both in standard as well as in an ultra-low-dose protocol with a tenfold decrease in dose. The detection rate reached 100% depending on a narrow slice thickness, thus suggesting that MDCTC should be performed with the least possible slice collimation (Fig. 2).

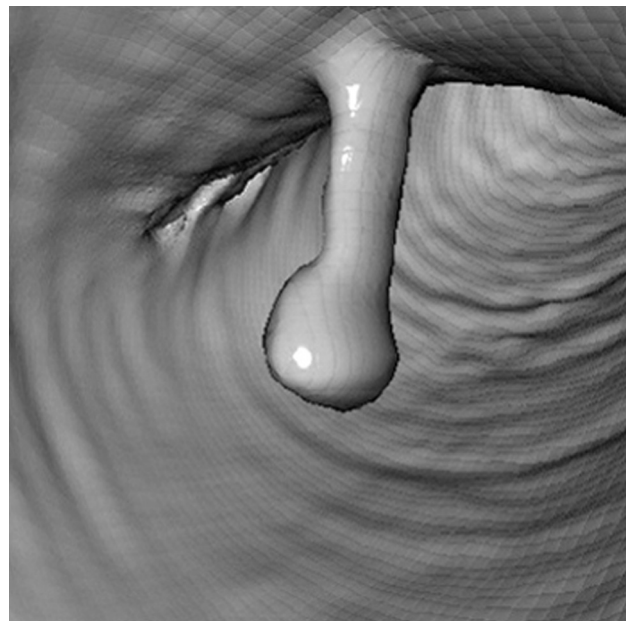


Fig. 2. Endoluminal view of a spheric lesion (long stalk).

In the present study, slice thickness exerted a major influence on the detection rate of artificial lesions in a phantom pig colon. With increasing slice thickness, the detection rate deteriorated from 100% to 89%. This phenomenon attributed to a reduced volume averaging has been demonstrated previously for single-row spiral CT [1, 20, 21]. A recent study proved that a slice thickness of 3 mm is favorable in terms of detection rate and lesion contrast compared to 5 or 7 mm slice thickness [22]. In the present study, even small artificial lesions of 1 mm size were detected with a reconstructed slice thickness of 1.25 mm.

This was true both for normal-dose as well as for the ultra-low-dose protocols after a mathematical noise reduction using a non-linear Gaussian filter [23, 24]. In contrast to filter mechanisms of the raw data matrix, the presented mathematical filter is applied to fully reconstructed DICOM-CT-images [25]. For the phantom used in this study, a reduction of noise in filtered images of up to 80% could be shown using ROI measurements preserving the air-lesion contrast.

For single-row spiral CT, higher pitch factors up to 2 seem beneficial both in terms of lowering dose as well as preserving a high lesion contrast at a minimal slice thickness [20-22, 26]. As pitch in MDCT is not as important as in single-row spiral CT, we did not systematically change pitch factors. In the present study, multi-slice pitch factors varied between 8 and 12.5, which correspond to "classical" pitch factors varying from 1.25 to 2.

For low-contrast lesions, a direct relation between dose and detectability or conspicuity is known as image noise increases when dose is reduced [27-29]. In imaging of high-contrast structures, however, it has already been shown both for single-row spiral CT and MDCT that a significant dose reduction may be achieved [8,30-35]. Thus it seems feasible to decrease dose in MDCTC similarly to low-dose CT of the chest, as endoluminal lesions like polyps or tumors show a high contrast to the surrounding colonic air or gas acting as negative contrast agent. Nevertheless ultra-low-dose as well as thin-slice protocols result in an increased image noise which could possibly prevent the detection of small or flat lesions [36, 37]. Thus, some authors require the lowest achievable noise for optimal detection [36]. The use of noise reduction filter algorithms as used in this study could be an interesting means to solve this problem. However, the shape of artificial lesions was more accurately delineated using normal dose protocols. This effect was most pronounced for thin slice protocols.

The display mode did not influence the detection rate in the presented in-vitro model. Only in one case (1x1 mm lesion in protocol III and IV), the detailed analysis of 2D-images and 3D-multiplanar reconstructions was superior to 3D-endoluminal views. However, as a slice collimation of 1 mm was used to create a 3 mm slice thickness, this protocol seems not feasible for clinical routine as dose in terms of CTDI or DLP does not differ from protocols I or II with a 1.25 mm slice thickness.

Minor stair-step artifacts were seen in all protocols. Images with a 3 mm slice thickness (protocols III/V) were rated to reveal moderate stair-step artifacts. Pre-

vious work shows that these artifacts depend on slice collimation and pitch [38]. They are minimized in thin slices and are pronounced with increasing pitch. However, in comparison to single-row spiral CT, stair-step artifacts are less prominent in MDCT [38].

The automated "polyp detector" used in this in-vitro model was programmed to mark any lesion larger than 3 voxel protruding into the lumen with an acute angle to the surrounding surface. No lesion of 1 or 2 mm size therefore was marked. The flat lesions either were not marked as they did not show acute but rectangular angles or even a slope. Thus, from a theoretical-mathematical point-of-view the automated system performed as intended. The further development of such computer aided diagnosis systems may help in improving the sensitivity as smaller lesions may be highlighted that might have been missed on visual assessment only [10, 39]. From a medical point-of-view, it remains to the medical personnel to interpret any marked lesion as well as check meticulously for other important lesions.

The main limitation of this phantom experiment is its in-vitro character. Any uncontrollable influence like motion artifacts, insufficient dilation of the colon, residual fluid or feces were excluded. Therefore, the results of this study can not be transferred directly to clinical routine. However, the data may serve as a basis on further discussion as to how a standard examination protocol for CT-colonography may probably be defined. Furthermore, no haustral folds or other probably disease-related changes of the mucosal surface impeded the diagnostic assessment. As the two colons measured approximately 20- and 25-inch, some bends and loops were arbitrarily created.

The use of a CT-scanner with four detector rows may be arguable in view of modern scanners with up to sixty-four detector rows, however, it remains to be cleared if a further reduction in slice thickness is of a major advantage in view of improved lesion detection [40, 41].

As has been shown previously, MDCTC has a high potential in the detection of endoluminal polyps and colonic tumors both in the symptomatic as well as in the asymptomatic patient [1-4,42-45]. It is a non-invasive method without complication and a high patient acceptance [46, 47]. As patient radiation exposure still constitutes an important limiting factor, thin-slice and ultra-low-dose protocols with high spatial resolution and low radiation exposure may result in images suffering from an increased image noise possibly preventing lesion detection [36, 37]. To reduce the increased noise without affecting spatial resolution or radiation dose, the use of noise reduction filter algorithms could be of decisive advantage. Further evaluation of ultra-low-dose CT-colonography is necessary to assess its feasibility in terms of sensitivity and specificity in-vivo particularly as a screening tool.

In conclusion, the in-vitro model suggests that MDCTC should be performed with a thin slice collimation of 4 x 1 mm in order to allow for detection of very small endoluminal lesions even below 5 mm size. A significant dose reduction may be possible as high contrast structures are imaged and mathematical filter methods exist to minimize image noise maintaining lesion contrast.

## REFERENCES

1. Dachman AH, Kuniyoshi JK, Boyle CM, et al. CT colonography with three-dimensional problem solving for detection of colonic polyps. *AJR Am J Roentgenol* 1998; 171(4): 989-995.
2. Fenlon HM, Nunes DP, Schroy PC, 3rd, et al. A comparison of virtual and conventional colonoscopy for the detection of colorectal polyps. *N Engl J Med* 1999; 341(20): 1496-1503.
3. Hara AK, Johnson CD, Reed JE, et al. Detection of colorectal polyps by computed tomographic colography: feasibility of a novel technique. *Gastroenterology* 1996; 110(1): 284-290.
4. Rex DK. Virtual colonoscopy: time for some tough questions for radiologists and gastroenterologists. *Endoscopy* 2000; 32(3): 260-263.
5. Fenlon HM. Colorectal neoplasm detection using virtual colonoscopy: a feasibility study. *Gastrointest Endosc* 2000; 51(3): 369-371.
6. Johnson CD, Hara AK, Reed JE. Computed tomographic colography (Virtual colonoscopy): a new method for detecting colorectal neoplasms. *Endoscopy* 1997; 29(6): 454-461.
7. Macari M, Green JC, Berman P, et al. Diagnosis of familial adenomatous polyposis using two-dimensional and three-dimensional CT colonography. *AJR Am J Roentgenol* 1999; 173(1): 249-250.
8. Schoepf UJ, Becker CR, Obuchowski NA, et al. Multislice computed tomography as a screening tool for colon cancer, lung cancer and coronary artery disease. *Eur Radiol* 2001; 11(10): 1975-1985.
9. Rogalla P, Meiri N, Ruckert JC, et al. Colonography using multislice CT. *Eur J Radiol* 2000; 36(2): 81-85.
10. Nicholson FB, Taylor S, Halligan S, Kamm MA. Recent developments in CT colonography. *Clin Radiol*. 2005 Jan;60(1):1-7.
11. Van Gelder RE, Nio CY, et al. Computed tomographic colography compared with colonoscopy in patients at increased risk for colorectal cancer. *Gastroenterology*. 2004 Jul;127(1):41-8.
12. Laghi A, Iannaccone R, Mangiapane F, et al. Experimental colonic phantom for the evaluation of the optimal scanning technique for CT colonography using a multidetector spiral CT equipment. *Eur Radiol* 2003 Mar;13(3):459-66
13. Hara AK, Johnson CD, MacCarty RL, et al. CT colonography: single- versus multi-detector row imaging. *Radiology* 2001; 219(2): 461-465.
14. Rust GF, Eisele O, Hoffmann JN, et al. [Virtual coloscopy with multi-slice computerized tomography. Preliminary results]. *Radiologe* 2000; 40(3): 274-282.
15. Wessling J, Fischbach R, Domagk D, et al. Colorectal polyps: Detection with multi-slice CT colonography. *Fortschr Rontgenstr* 2001; 173(12): 1069-1071.
16. van Gelder RE, Venema HW, Serlie IW, et al. CT colonography at different radiation dose levels: feasibility of dose reduction. *Radiology* 2002; 224(1): 25-33.
17. Summers RM, Johnson CD, Pusanik LM, et al. Automated polyp detection at CT colonography: feasibility assessment in a human population. *Radiology* 2001; 219(1): 51-59.
18. Yoshida H, Masutani Y, MacEneaney P, et al. Computerized Detection of Colonic Polyps at CT Colonography on the Basis of Volumetric Features: Pilot Study. *Radiology* 2002; 222(2): 327-336.
19. Aurich V, Winkler G, Hahn K, et al. Noise Reduction in Images: some recent Edge-Preserving Methods. *Pattern Recognition and Image Analysis* 1999; 9(4): 749-766.
20. Beaulieu CF, Napel S, Daniel BL, et al. Detection of colonic polyps in a phantom model: implications for virtual colonoscopy data acquisition. *J Comput Assist Tomogr* 1998; 22(4): 656-663.
21. Springer P, Stohr B, Giacomuzzi SM, et al. Virtual computed tomography colonoscopy: artifacts, image quality and radiation dose load in a cadaver study. *Eur Radiol* 2000; 10(1): 183-187.
22. Power NP, Pryor MD, Martin A, et al. Optimization of scanning parameters for CT colonography. *Br J Radiol* 2002; 75(893): 401-408.
23. Aurich V, Winkler G, Liebscher V. Probabilistic Image Smoothing: Recent Advances. *International Conference on Stereology, Spatial Statistics and Stochastic Geometry, Prague. Union of Czech Mathematicians and Physicists, 1999; 273-278.*
24. Aurich V, Weule J. Non-linear Gaussian Filters Performing Edge Preservation Diffusion. 17. DAGM-Symposium, Bielefeld. Springer, 1995; 538-545.
25. Kachelriess M, Watzke O, Kalender WA. Generalized multi-dimensional adaptive filtering for conventional and spiral single-slice, multi-slice, and cone-beam CT. *Med Phys* 2001; 28(4): 475-490.
26. Schorn C, Obenauer S, Funke M, et al. [Slice sensitivity profile and image pixel noise of multi-slice spiral CT in comparison with single slice spiral CT]. *Fortschr Rontgenstr* 1999; 171(3): 219-225.
27. Cohnen M, Fischer H, Hamacher J, et al. CT of the head by use of reduced current and kilovoltage: relationship between image quality and dose reduction. *AJNR Am J Neuroradiol* 2000; 21(9): 1654-1660.
28. Jurik AG, Jessen KA, Hansen J. Image quality and dose in computed tomography. *Eur Radiol* 1997; 7(1): 77-81.
29. Scheck RJ, Coppentrath EM, Kellner MW, et al. Radiation dose and image quality in spiral computed tomography: multicentre evaluation at six institutions. *Br J Radiol* 1998; 71(847): 734-744.
30. Cohnen M, Cohnen B, Koch JA, et al. [Possibilities for dose reduction in coronal spiral CT of the mid-face area]. *Aktuelle Radiol* 1998; 8(1): 34-39.
31. Diederich S, Lenzen H, Windmann R, et al. Pulmonary nodules: experimental and clinical studies at low-dose CT. *Radiology* 1999; 213(1): 289-298.
32. Diederich S, Wormanns D, Lenzen H, et al. Screening for asymptomatic early bronchogenic carcinoma with low dose CT of the chest. *Cancer* 2000; 89(11 Suppl): 2483-2484.
33. Husstedt HW, Prokop M, Dietrich B, et al. Low-dose high-resolution CT of the petrous bone. *J Neuroradiol* 2000; 27(2): 87-92.
34. Jung KJ, Lee KS, Kim SY, et al. Low-dose, volumetric helical CT: image quality, radiation dose, and usefulness for evaluation of bronchiectasis. *Invest Radiol* 2000; 35(9): 557-563.
35. Iannaccone R, Laghi A, et al. Computed tomographic colography without cathartic preparation for the detection of colorectal polyps. *Gastroenterology*. 2004 Nov;127(5):1300-11.
36. Johnson KT, Johnson CD, Anderson SM, Bruesewitz MR, Mccollough CH. CT colonography: determination of optimal CT technique using a novel colon phantom. *Abdom Imaging*. 2004 Mar-Apr;29(2):173-6.
37. Özgün A, Rollven E, Blomqvist L, et al. Polyp detection with MDCT: a phantom-based evaluation of the impact of dose and spatial resolution. *AJR Am J Roentgenol*. 2005 Apr;184(4):1181-8.
38. Fleischmann D, Rubin GD, Paik DS, et al. Stair-step artifacts with single versus multiple detector-row helical CT. *Radiology* 2000; 216(1): 185-196.
39. Summers RM, Beaulieu CF, Pusanik LM, et al. Automated polyp detector for CT colonography: feasibility study. *Radiology* 2000; 216(1): 284-290.

40. Pickhardt PJ, Taylor AJ, Johnson GL, Fleming LA, Jones DA, Pfau PR, Reichelderfer M. Building a CT colonography program: necessary ingredients for reimbursement and clinical success. *Radiology* 2005 Apr; 235(1):17-20.
41. Park SH, Ha HK, Kim MJ, et al. False-negative results at multi-detector row CT colonography: multivariate analysis of causes for missed lesions. *Radiology*. 2005 May; 235(2):495-502. Epub 2005 Mar 15.
42. Ferrucci JT. Colon cancer screening with virtual colonoscopy: promise, polyps, politics. *AJR Am J Roentgenol* 2001; 177(5): 975-988.
43. Fletcher JG, Johnson CD, Krueger WR, et al. Contrast-Enhanced CT Colonography in Recurrent Colorectal Carcinoma: Feasibility of Simultaneous Evaluation for Metastatic Disease, Local Recurrence, and Metachronous Neoplasia in Colorectal Carcinoma. *AJR Am J Roentgenol* 2002; 178(2): 283-290.
44. Johnson CD, Ahlquist DA. Computed tomography colonography (virtual colonoscopy): a new method for colorectal screening. *Gut* 1999; 44(3): 301-305.
45. Pickhardt PJ et al.: Computed tomographic virtual colonoscopy to screen for colorectal neoplasia in asymptomatic adults. *N Engl J Med*. 2003 Dec 4; 349(23):2191-200
46. Farrell RJ, Morrin MM, McGee JB. Virtual colonoscopy: a gastroenterologist's perspective. *Dig Dis* 1999; 17(4): 185-193.
47. Svensson MH, Svensson E, Lasso A, et al. Patient Acceptance of CT Colonography and Conventional Colonoscopy: Prospective Comparative Study in Patients with or Suspected of Having Colorectal Disease. *Radiology* 2002; 222(2): 337-345.

*Received: November 17, 2005 / Accepted: November 30, 2005*

*Address for correspondence:*

Priv.-Doz. Dr. med. M. Cohnen  
Institute of Diagnostic Radiology  
University Hospital Düsseldorf  
MNR-Klinik  
Moorenstr. 5.  
D-40225 Duesseldorf, Germany  
Tel.: ++49-211-8117752  
Fax: ++49-211-8116145  
e-mail: cohnen@med.uni-duesseldorf.de